



Article

Assessment of Water Yield and Water Purification Services in the Arid Zone of Northwest China: The Case of the Ebinur Lake Basin

Xilinayi Duolaiti ^{1,2}, Alimujiang Kasimu ^{1,2,3,*} , Rukeya Reheman ^{1,2}, Yimuranzi Aizizi ^{1,2} and Bohao Wei ^{1,2} 

¹ School of Geography and Tourism, Xinjiang Normal University, Urumqi 830054, China

² Xinjiang Key Laboratory of Lake Environment and Resources in Arid Zone, Urumqi 830054, China

³ Research Centre for Urban Development of Silk Road Economic Belt, Xinjiang Normal University, Urumqi 830054, China

* Correspondence: alimkasim@xjnu.edu.cn; Tel.: +86-150-9907-9321

Abstract: Assessing how land-use changes will affect water-producing ecosystem services is particularly important for water resource management and ecosystem conservation. In this study, the InVEST model and geographical detector were used to assess the water ecosystem service functions of the Ebinur Lake Basin and analyze their relationship with land-use changes. The results show that in the past 25 years, the water yield of the study area showed a trend of a strong yield at first and then a weaker one; there was a relatively large water yield in the west and southeast regions of the basin. The order of water yield for different land-use types is as follows: forest land > grassland > water area > unused land > crop land > construction land. After 2010, the output load of nitrogen and phosphorus increased; thus, the water purification ability weakened. The main land-use types in areas that demonstrate a large change rate in water purification capacity in the basin are cultivated land and construction land. Changes in the two water ecosystem services were associated with land-use changes. Geodetector analysis results further validated this conclusion. This study proposes a viable, replicable framework for land-use decisions in ecologically fragile watersheds. This study not only helps to gain insight into urban growth patterns in the study area but also helps to inform different land-use stakeholders.

Keywords: Ebinur Lake Basin; water yield; water purification; InVEST model; geographical detector



Citation: Duolaiti, X.; Kasimu, A.; Reheman, R.; Aizizi, Y.; Wei, B. Assessment of Water Yield and Water Purification Services in the Arid Zone of Northwest China: The Case of the Ebinur Lake Basin. *Land* **2023**, *12*, 533. <https://doi.org/10.3390/land12030533>

Academic Editors: Alim Samat, Anming Bao, Jingjie Wang, Zhi Li, Xuemei Li, Ali Darvishi Bolorani and Mukhiddin Juliev

Received: 16 January 2023

Revised: 19 February 2023

Accepted: 20 February 2023

Published: 22 February 2023



Copyright: © 2023 by the authors. Licensee MDPI, Basel, Switzerland. This article is an open access article distributed under the terms and conditions of the Creative Commons Attribution (CC BY) license (<https://creativecommons.org/licenses/by/4.0/>).

1. Introduction

Water is an essential resource for human survival and an important condition for the sustainable development of regional economies and ecosystems [1]. With the acceleration of human production and urbanization, the demand for water resources is also increasing rapidly. At the same time, the environmental pollution of water and water shortages that are caused by human activities are becoming more and more serious [2]. The magnitude of global desalination water production, which is the total water produced by desalination technology globally, provides critical information on the research and application of global desalination technology and its contribution to mitigating the water shortage issue [3]. Therefore, the study of the spatial and temporal distribution and change in water yield and water purification services is particularly important for the rational development and utilization of regional water resources. As the most important function of ecosystem services: water yield and water purification services play a key role in improving the hydrological conditions of watersheds and regulating the water cycle [4]. Water yield is the process and capacity of an ecosystem to store and hold water in a given time and space [5]. Non-rainy season drainage and recharge of the ecological base flow in a watershed ensure water for human life and social development [6]. Water purification services refer to the ability of an ecosystem to absorb, transform, and redistribute pollutants in a water

body through its own natural ecological processes and material cycles [7]. Therefore, the visualization and quantitative assessment of the spatial and temporal variation of water yield and water purification services in a watershed and their influencing factors have become a trend and a popular topic in the fields of ecology and hydrology [8]. This topic has an important application value and a guiding significance for the optimal allocation of water resources and the sustainable development of ecosystems in watersheds.

Due to the limitations of traditional methods in the number of monitoring stations and conditions of observation equipment, the large spatial scale estimation produces large significant errors [9]. Commonly used water quality evaluation methods can only evaluate the water quality of the river wetlands and other water quality conditions; it is not possible to estimate the water purification services of the ecosystem [10]. With the development and application of remote sensing and GIS technology, more models in the fields of ecology and hydrology can realize the simulation and evaluation of water yield and water purification services in a watershed. The main ones are the TOPMODEL model [11], the Xin'anjiang model [12], the SWAT model [13], the MIMES model [14], the SolVES model [15,16], the ARIES model [17], and the InVEST model [18]. Among them, the InVEST model has significant advantages in terms of low data requirements, easy access to a few parameters, quantification of spatial data, a scenario simulation function, and the visualization of results. The InVEST water yield module is based on the water balance principle. Water yield is calculated from precipitation, surface evaporation, plant transpiration, soil depth, and other parameters [19]. The water quality purification module uses nitrogen (N) and phosphorus (P) content to characterize the water quality status. The water quality purification function is achieved by reducing and removing N and P content through the storage and conversion of plants and soil [20]. In recent years, the InVEST model has become more widely applied in China and abroad. Mulatu et al. discussed the possibility of the Naivasha Lake basin development and water ecosystem service plan in Kenya [21]. Schmalz et al. assessed water ecosystem services in three lowland river basins in western Siberia [22]. Sun Xiaoyin et al. simulated the water yield of the South Four Lakes' watershed for nearly 25a based on the InVEST model. Additionally, ArcGIS was used to analyze the spatial distribution pattern of water yield and trend change. The relationship between natural geographic factors such as precipitation and topography; socio-economic factors such as population, land use, and gross domestic product (GDP); and the dynamic changes in the spatial pattern of water yield were explored [23]. Mei et al. analyzed the spatial and temporal variation of water purification in the Guan Hall reservoir watershed using the InVEST model; their study showed that water quality purification services in the watershed showed an increasing trend [24].

These studies provide a valuable reference for regional water resource management and ecological planning. We found that, in addition to considering the effects of land type conversion on changes in water ecosystem services, the factors influencing water-related ecosystem service functions in arid and semi-arid regions would help to more systematically and comprehensively assess the effects of land-use change on changes in regional water ecosystem services. The InVEST model enables effective assessment of the status of ecosystem services, and spatial the InVEST model can provide a valid assessment of ecosystem services and spatial analysis, providing valid and critical information for management decisions. However, detailed assessments of aquatic ecosystem services using this model are currently rare in arid regions.

River runoff from the Ebinur Lake Basin is the main source of irrigation in the north-western region of Xinjiang and the main water resource for maintaining the ecological balance of the entire Bortala Mongol Autonomous Prefecture, hence occupying an important social and ecological location. The region's main inlet rivers, the Jing River and the Bortala River, pass through areas such as Hot Spring County, Bole City, and Jinghe County. Water shortages and pollution are prominent in this ecosystem due to the influence of local land use and climate change. Based on the InVEST model and geographic probes, this study proposes a feasible and replicable framework for land-use decision-making in ecologically

fragile areas. This framework not only contributes to an in-depth understanding of urban growth patterns in the study area but also helps to inform different land-use stakeholders. The overall objective of this study is to assess the spatial and temporal patterns and evolutionary characteristics of water production and water purification services in the Lake Ebinur basin and to analyze their relationship to land-use change. The use of a geodetector model to explore the dominant drivers of changes to ecosystem water production and water purification is scientifically important for promoting ecosystem management and conservation in the northwest arid zone of China, alleviating increasingly serious water resource problems, and achieving sustainable development.

2. Study Area and Data Sources

2.1. Study Area

The Ebinur Lake Basin is located in the northwestern part of Xinjiang Uygur Autonomous Region. The geographical position of the study area is between 43°38' N to 45°52' N and 79°53' E to 85°02' E. It is surrounded by mountains on the west, north, and south, with the valley plain in the middle (Figure 1). It has a high land-surface temperature, arid continental climate: arid with little rain, high evaporation, and high wind and sand. It has an average annual temperature of 7.5 °C, an average annual precipitation of 105.17 mm, and an average annual evaporation of 1315 mm [25,26]. The river runoff from the Ebinur Lake Basin is the main source of irrigation in northwest Xinjiang and also the main water resource to maintain the ecological balance of the entire Boertala Mongolian Autonomous Prefecture, thus occupying an important social and ecological location in the region. This region includes the Jinghe River watershed in Bortala Mongol Autonomous Prefecture, the Bortala River watershed, and the Kuitun River watershed in the Yili Kazakh Autonomous Prefecture. Due to the recent population growth and intensification of water use for industrial and agricultural production activities, the water volume of the Ebinur Lake is decreasing. Thereby, most of Lake Ebinur's water recharge rivers are disconnected downstream, which has led to a rapid drying out of the water surface area of Lake Ebinur. As a result, the ecological security of the whole watershed is seriously affected. The gradual deterioration of the ecological environment in the Lake Ebinur watershed directly threatens the sustainable socio-economic development of the basin [26].

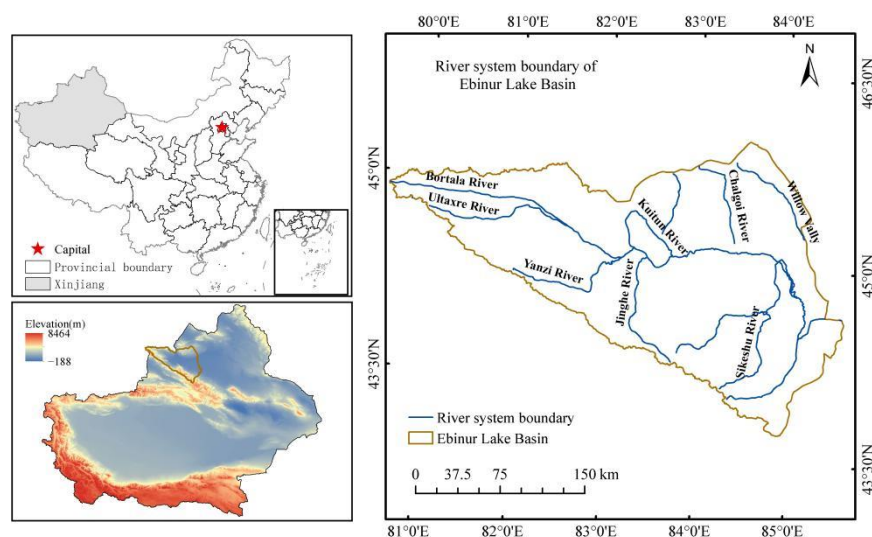


Figure 1. Schematic diagram of the Ebinur Lake Basin.

2.2. Data Sources and Research Methodology

The data involved in this study include land-use data, digital elevation data, meteorological data, potential evapotranspiration data, soil data, night-light data, and nitrogen and phosphorus output coefficient data. The land-use data were obtained from the Data Center

for Resource and Environmental Sciences (<https://www.resdc.cn/>, accessed on 15 January 2023, resolution 1 km) of the Chinese Academy of Sciences. Digital elevation data were provided by the Geospatial Data Cloud Platform (<http://www.gscloud.cn>, accessed on 15 January 2023). Meteorological data from 1995 to 2020, with 5-year time intervals, were obtained from the National Tibetan Plateau Scientific Data Center (<http://data.tpdac.ac.cn/>, accessed on 15 January 2023). The potential evapotranspiration was calculated using the Hargreaves formula. Socio-economic factors were selected from population density and GDP data (<https://www.resdc.cn/>, accessed on 15 January 2023). Soil data were obtained from the World Soil Database. NDVI data and nighttime light data were obtained using the Google Remote Sensing cloud computing platform. NDVI is the annual average data calculated by the MOD13Q11 km resolution product. Nighttime light data, 1995–2010, were DMSP/OLS data; 2015 and 2020 were NPP/VIIRS data. The above data were uniformly transformed into 1 km × 1 km raster data after a series of data pre-processing steps, such as projection transformation and cropping and resampling in GIS analysis software. The nitrogen and phosphorus output coefficients and removal efficiencies were obtained by the InVEST user guide for estimation (Table 1).

Table 1. Data sources and notes for this study.

| No | Datasets | Data | Data Resources |
|----|----------------------------|--|---|
| 1 | Land-use/cover datasets | Land-use/cover data | http://www.resdc.cn/data.aspx?DATAID=252 (accessed on 15 March 2022) |
| 2 | Vector datasets | Administrative district boundaries | https://xinjiang.tianditu.gov.cn (accessed on 15 March 2022) |
| 3 | Meteorological datasets | Average annual precipitation Average annual temperature potential evapotranspiration | http://data.tpdac.ac.cn (accessed on 15 March 2022) |
| 4 | Social datasets | Population Gross Domestic Product | http://www.resdc.cn/data.aspx?DATAID=252 (accessed on 20 January 2021) (https://www.resdc.cn/ accessed on 20 March 2022) |
| 5 | Road network datasets | Distance from railways Distance from motorways Distance from provincial roads Distance from county roads Distance to country roads | https://www.webmap.cn/main.domethod=index (accessed on 15 March 2022) calculated by Euclidean distance |
| 6 | Topographic factor dataset | Distance to water Elevation Slope | http://www.gscloud.cn/#page1/2- (accessed on 20 January 2021) |
| 7 | Impact factor dataset | Nighttime lighting index Normalized-difference vegetation index Normalized-difference building soil index | GEE (accessed on 15 March 2022) MODISTerra vegetation index data MYD13A1 16-day products MODISAqua surface reflectance data MYD09A1 8-day products |
| 8 | Soil datasets | Clay, silt, sand | HWSD v1.2 |

2.3. Research Methodology

In this study, first of all, the multi-source data set: land-use data, digital elevation data, meteorological data, and potential evapotranspiration data were preprocessed for achieving the study's requirement. Secondly, after the data were pre-processed, the annual water yield and purification were calculated based on the InVEST model. The framework of this study is presented in Figure 2.

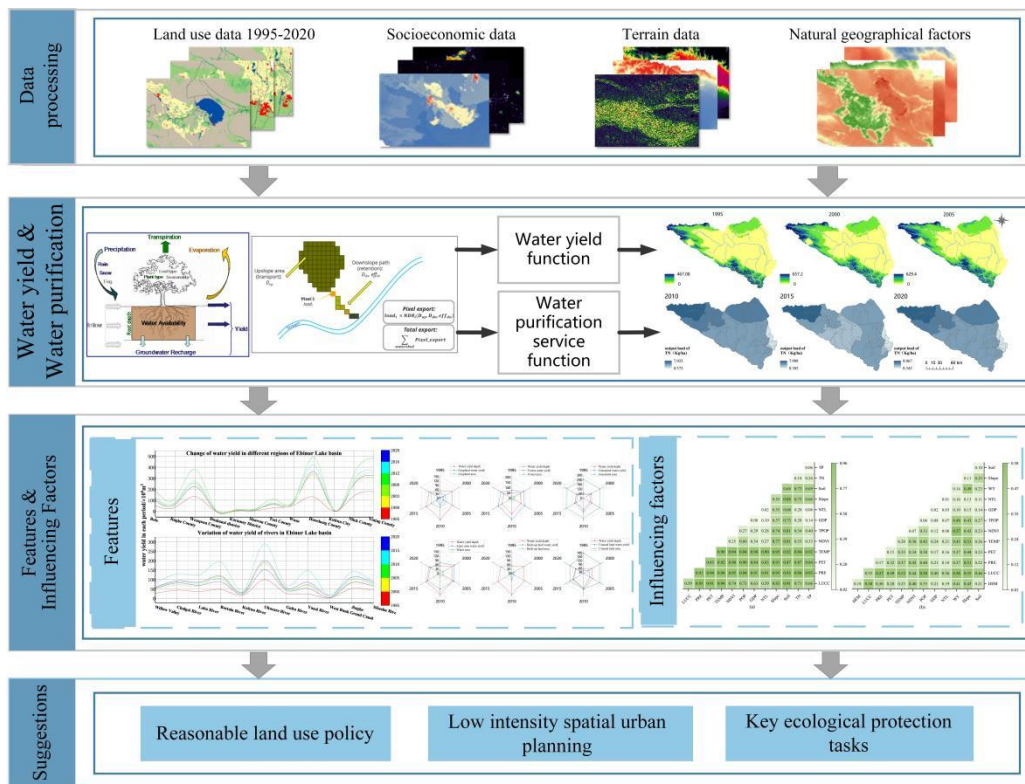


Figure 2. The research process of this study.

2.3.1. Spatial and Temporal Land-Use Changes and Scenario Simulations

The land-use type transfer matrix is derived from systems analysis, which is a quantitative process of analyzing and studying the state of a system and the amount of transfer: the area transferred out and the area transferred in [27,28]. The analysis can be expressed in terms of land-use transfer area or transfer probability [28]. This calculation formula is as follows:

$$T_1 = \begin{bmatrix} S_{11} & S_{12} & \dots & S_{1n} \\ S_{21} & S_{22} & \dots & S_{2n} \\ \vdots & \vdots & \vdots & \vdots \\ S_{n1} & S_{n2} & \dots & S_{nn} \end{bmatrix} \text{ or } T_2 = \begin{bmatrix} P_{11} & P_{12} & \dots & P_{1n} \\ P_{21} & P_{22} & \dots & P_{2n} \\ \vdots & \vdots & \vdots & \vdots \\ P_{n1} & P_{n2} & \dots & P_{nn} \end{bmatrix} \quad (1)$$

where T_1 and T_2 are two representations of the land-use transfer matrix for the studied time period. T_2 is known as the transfer probability matrix; S_{ij} is the probability of transfer from land class i transferred to land class j of the area; P_{ij} is the type of land use i transferred from the land class at the beginning of the study to the land class at the end of the study; n is the number of land-use types.

2.3.2. Assessment of Water Production

Water yield is calculated by estimating the amount of water that falls in each grid cell minus the actual evapotranspiration [29,30]. The formula is as follows:

$$Y_x = \left(1 - \frac{AET_x}{P_x} \right) \times P_x \quad (2)$$

where Y_x denotes the grating cell's x annual water yield (m^3 /year); AET_x denotes the x Annual actual evapotranspiration (mm/year); P_x denotes the annual precipitation of the grid cell x (mm/year); and vegetation evapotranspiration is determined by land use/cover

type $\frac{AET_x}{P_x}$. The equation of Budyko's [30] water-heat coupling equilibrium assumption was used to calculate the formula:

$$\frac{AET_x}{P_x} = \frac{1 + \omega R_{(x,j)}}{1 + \omega R_{(x,j)} + 1/R_{(x,j)}} \quad (3)$$

where $R_{(x)}$ is the dimensionless drying index of grid cell x ; $\omega_{(x)}$ is a dimensionless nonphysical parameter representing soil properties under natural climate conditions, defining the curve shape related to potential evapotranspiration, which is calculated by Equations (2) and (3):

$$R_x = \frac{K_C - ET_{0x}}{p_x} \quad (4)$$

$$W_x = \frac{AWC_x \times Z}{P_x} + 1.25$$

where k_c represents the crop coefficient of crop evapotranspiration; ET_{0x} reference evapotranspiration of x grid cell; and Z is an empirical parameter, which can represent regional precipitation distribution and other hydrogeology. The characteristic value range is 1–30. AWC_x is vegetation water content in mm, the calculation formula is as follows:

$$AWC_x = \min(\text{soil_depth}, \text{root_depth}) \times PAWC \quad (5)$$

where $PAWC$ is the plant available water; the nonlinear fitting model based on soil texture and soil organic matter, the values range from 0 to 1. The formula proposed by Wenzhou [31–33] was used to calculate by following formula:

$$PAWC = 54.509 - 0.132 \text{ Sand}\% - 0.003 (\text{Sand}\%)^2 - 0.055 \times \text{Silt}\% - 0.006 \times (\text{Silt}\%)^2 - 0.738 \times \text{Clay}\% + 0.007 \times (\text{Clay}\%)^2 - 2.688 \times \text{OM}\% + 0.501 \times (\text{OM}\%)^2 \quad (6)$$

where $\text{Sand}\%$ is the soil sand content; $\text{Silt}\%$ is the soil powder content; $\text{Clay}\%$ is the soil clay content; and $\text{OM}\%$ is the soil organic matter content.

The model was set up with parameters for different root depths based on different land-use data and the "Guide to Calculating Crop Evapotranspiration—Crop Water Requirements." Reference values for evapotranspiration coefficients (k_c were set up according to the Food and Agriculture Organization of the United Nations (FAO) to obtain the biophysical parameters needed for this study. The water yield assessment and validation process was as follows: through comparison with the water resources bulletin, iterative experiments were conducted to obtain the simulated values closest to the real values, and then the final input parameters for the model were obtained based on these results. The government water resources bulletin shows that the surface water resource in Xinjiang in 2010 was $1063 \times 10^6 \text{ m}^3$. The modal water yield was calculated from the water resources bulletin and when $Z = 1$, the modelled value for 2010 was $891 \times 10^6 \text{ m}^3$, which was the closest to the actual value. Therefore, this value was used as the basis for the next step of analysis in this study.

2.3.3. Assessment of Water Quality Purification

The water quality purification module of the InVEST model is based on the mechanism by which vegetation and soil can convert or store nitrogen and phosphorus pollutants in runoff [32]. Ignoring other sources of pollution, the levels of total nitrogen and total phosphorus in the water body were used to represent the water quality condition of the watershed. The greater the content of total nitrogen and total phosphorus, the more serious the pollution in the basin and the weaker its ability to purify water [34]. The calculation formula is as follows:

$$ALV_x = HSS_x \times pol_x \quad (7)$$

where ALV_x represents the regulated load value of raster cell x ; pol_x represents the output coefficient of raster cell x . HSS_x is the hydrological sensitivity of raster cell x , the calculation is as follows:

$$HSS_x = \gamma_x \sqrt{\gamma_\omega} \tag{8}$$

where γ_x denotes the raster cell x of the runoff coefficient; $\sqrt{\gamma_\omega}$ denotes the runoff coefficient of the evaluation in the watershed.

2.3.4. Geographical Detector

Detection of spatial differentiation is one of the core features of the geographical detector, a novel statistical method that can reveal the driving force behind habitat quality [35,36]. It can effectively discern spatially stratified heterogeneity among variable factors (Figure 3) [37,38]. The factor detector can measure the spatial and temporal heterogeneity of different factors on habitat quality as well as detect the magnitude of their influence. As shown in the following equation:

$$q = 1 - \frac{\sum_{h=1}^L N_h \sigma_h^2}{N \sigma^2} \tag{9}$$

where q is the degree of influence of a factor; L is the number of samples of the influence factor; N_h and N are the number of units in layer h and the whole area, respectively. The value interval of q is $(0, 1)$, the larger the value, the more obvious the spatial differentiation of Y [39]. Interaction detection is used to judge the interaction between different influencing factors, that is, to evaluate whether the explanatory power of the dependent variable will increase or decrease when the factors $X1$ and $X2$ act together [40,41]. The relationship between the two factors can be divided into the categories described in Table 2.

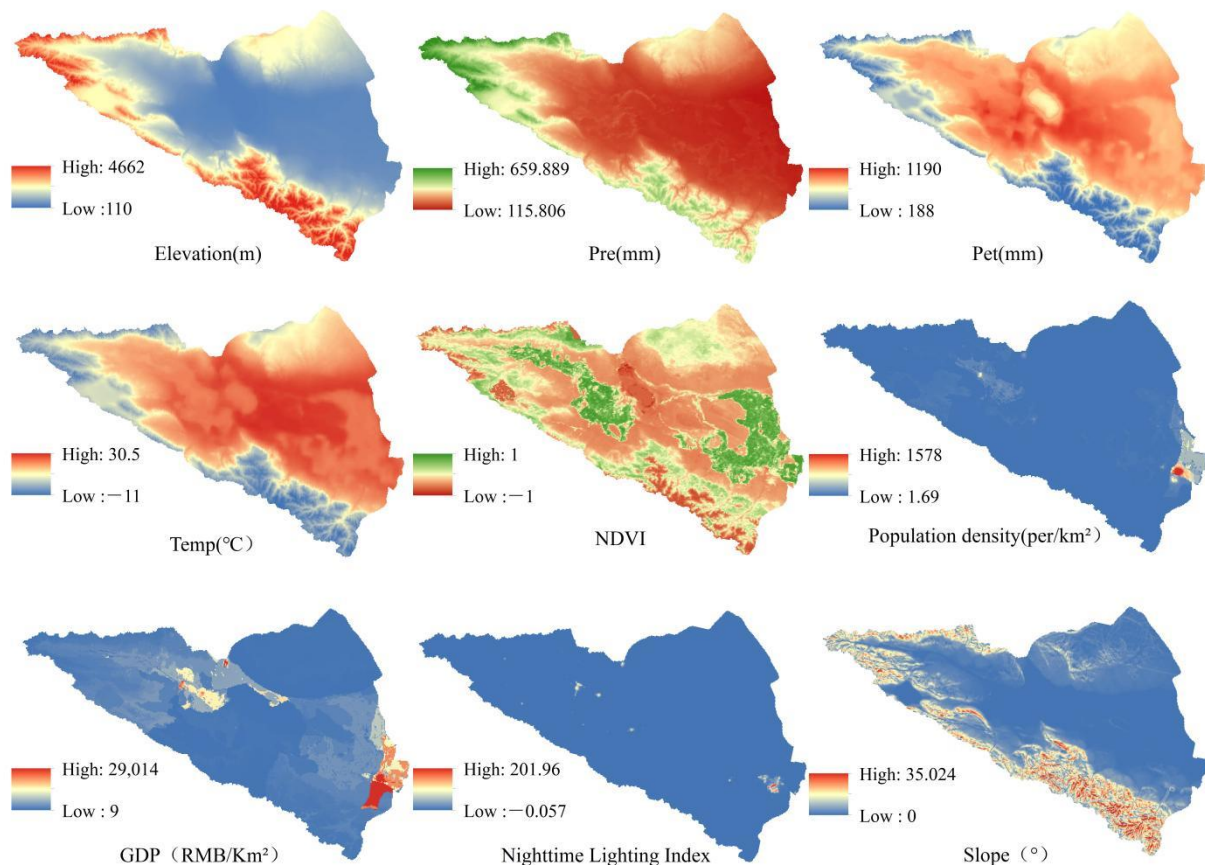


Figure 3. Map of impact factors for future land-use projections.

Table 2. Types of two-factor interaction result.

| Criterion | Interaction |
|---|--------------------------------------|
| $q(X1 \cap X2) < \text{Min}(q(X1), q(X2))$ | Non-linear attenuation |
| $\text{Min}(q(X1), q(X2)) < q(X1 \cap X2) < \text{Max}(q(X1), q(X2))$ | Single factor non-linear attenuation |
| $q(X1 \cap X2) > \text{Max}(q(X1), q(X2))$ | Two-factor enhancement |
| $q(X1 \cap X2) = q(X1) + q(X2)$ | Independent |
| $q(X1 \cap X2) > q(X1) + q(X2)$ | Non-linear enhancement |

3. Results and Analysis

3.1. Spatial and Temporal Changes of Land Use in the Ebinur Lake Basin

The land-use structure of the Ebinur Lake Basin from 1995 to 2020 is dominated by grassland, unused land, and cropland (Figure 4). The annual average area proportions are 49.97%, 30.89%, and 11.06%, respectively. Next, the land-use structure is followed by water area and forest land, which account for 3.49% and 3.77%, respectively. The built-up land only accounted for 0.77%. In terms of dynamic attitude and rate of change, the built-up land area increased the most. It increased from 159.84 km² to 612.08 km², an increase of about 282.93%, whereas the dynamic attitude increased by 11.32%. The next largest change was in cropland, with a rate of change of 96.29%. The dynamic attitude is 3.85%. Grassland has the smallest increase, from 24,538.88 km² to 25,765.82 km². The area of forest land, unused land, and water area is decreasing. Among them, forest land decreased the most, reaching −48.28%. The area of unused land decreased from 2185.67 km² to 1130.49 km², a decrease of −21.03%. The rate of change in water area is −15.8% (Table 3).

Table 3. Land-use area percentage and dynamic degree in the Ebinur Lake Basin from 1995 to 2020.

| Land-Use Type | Proportional Change of Different Land-Use Types/% | | | | | | 1995–2020 Rate of Change/% | Dynamic of Single Land Use/% |
|---------------|---|-------|-------|-------|-------|-------|----------------------------|------------------------------|
| | 1995 | 2000 | 2005 | 2010 | 2015 | 2020 | | |
| Cropland | 7.35 | 8.14 | 9.31 | 12.92 | 14.41 | 14.42 | 96.29 | 3.85 |
| Forest | 4.35 | 4.81 | 4.82 | 2.44 | 2.28 | 2.25 | −48.28 | −1.93 |
| Grassland | 48.81 | 48.43 | 47.54 | 52.48 | 51.34 | 51.25 | 5.00 | 0.20 |
| Water area | 3.92 | 4.48 | 4.72 | 3.18 | 3.07 | 3.30 | −15.80 | −0.63 |
| Built-up land | 0.32 | 0.51 | 0.58 | 0.91 | 1.09 | 1.22 | 282.93 | 11.32 |
| Unused land | 35.26 | 33.63 | 33.02 | 28.08 | 27.81 | 27.56 | −21.83 | −0.87 |

The largest transferred-in and transferred-out areas were grassland and unused land, followed by cropland (Figure 4). Among them, the transferred area of grassland reached 25,763.4 km². The main sources of transfer were unused land and forest land. The percentages of transferred-in area were 17.38% and 4.38%, respectively. The transferred-out area of grassland was 24,535.42 km². The main transfer-out area was cropland with 2502.68 km². The transfer-out area of unused land reaches 17,720.36 km². The main transfer-out area was grassland, with a percentage of 25.26%. This area was followed by cropland with 6.8%, which indicates that a larger development and utilization of unused land was carried out. The area transferred from cropland reached 7249.59 km². The main source of transfer was grassland, followed by unused land. There was a mutual transfer between unused land, grassland, and cropland (Table 4). The largest transferred-out area of the water area was unused land.

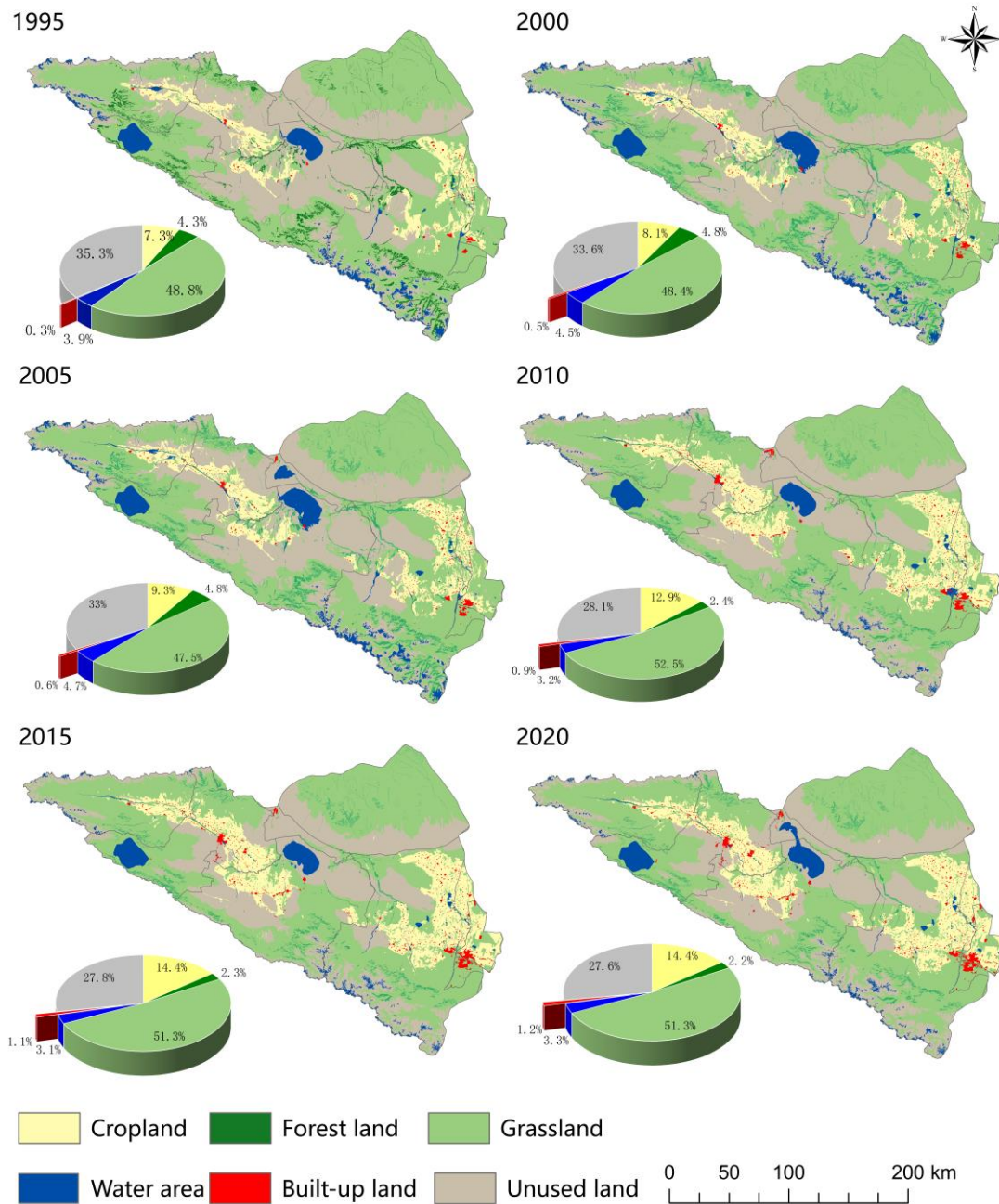


Figure 4. Distribution map of land-use change of the Ebinur Lake Basin from 1995 to 2020.

In terms of an overall perspective, during 1995–2020, the land-use types in the study area were characterized by “two increases, two decreases and two stabilizations.” The “two increases” refer to the increasing trend of the area of arable land and construction land during the study period; the “two decreases” refer to the decreasing trend of the area of forest land and unused land during the study period; the “two stabilizations” refer to the area of the watershed and grassland that remained mostly stable during the study period. Spatially, the change was greater in the south-east, as arable land in the east is expanded towards the south of the study area. This area is mainly located in the plain cultivation zone, where human activities are relatively frequent, and alongside urban and rural settlement areas, bare land, and low-coverage grassland, so the land-use changes in this area are more evident.

The rows in the table represent i land-use types in 1995, and the columns represent j land-use types in 2020; A represents the area where the land-use type in 1995 was trans-

formed into the land-use type in 2020, i.e., the original transfer matrix T; B (%) represents i land-use types as a percentage of area transferred out in 1995; C (%) represents j land-use types as a percentage of transferred area in 2020.

Table 4. Land-use transfer area and proportion in the Ebinur Lake Basin during 1995–2020.

| 1995 | 2020 Year | | | | | | Area of Transfer Out | |
|---------------------|-----------|---------|-----------|----------|---------------|-------------|----------------------|-----------|
| | Cropland | Forest | Grassland | Water | Built-Up Land | Unused Land | | |
| Cropland | A | | 17.75 | 162.31 | 14.65 | 196.83 | 4.84 | 3693.28 |
| | B | | 0.48 | 4.39 | 0.40 | 5.33 | 0.13 | |
| | C | | 1.57 | 0.63 | 0.88 | 32.16 | 0.03 | |
| Forest | A | 185.42 | | 1243.99 | 17.47 | 7.61 | 105.09 | 2182.52 |
| | B | 8.50 | | 57.00 | 0.80 | 0.35 | 4.82 | |
| | C | 2.56 | | 4.83 | 1.05 | 1.24 | 0.76 | |
| Grassland | A | 2502.68 | 447.01 | | 78.1 | 194.33 | 1558.79 | 24,535.42 |
| | B | 10.20 | 1.82 | | 0.32 | 0.79 | 6.35 | |
| | C | 34.52 | 39.55 | | 4.71 | 31.75 | 11.26 | |
| Water | A | 16.09 | 2.76 | 122.35 | | 1.97 | 560.41 | 1968.51 |
| | B | 0.82 | 0.14 | 6.22 | | 0.10 | 28.47 | |
| | C | 0.22 | 0.24 | 0.47 | | 0.32 | 4.05 | |
| Built-up land | A | 42.94 | 0.02 | 3.34 | 0.32 | | 2.45 | 159.84 |
| | B | 26.86 | 0.01 | 2.09 | 0.20 | | 1.53 | |
| | C | 0.59 | 0.00 | 0.01 | 0.02 | | 0.02 | |
| Unused land | A | 1205.55 | 39.87 | 4476.73 | 281.50 | 100.56 | | 17,720.36 |
| | B | 6.80 | 0.23 | 25.26 | 1.59 | 0.57 | | |
| | C | 16.63 | 3.53 | 17.38 | 16.99 | 16.43 | | |
| Area of transfer in | | 7249.59 | 1130.35 | 25,763.2 | 1656.96 | 612.075 | 13,847.7 | 50,259.9 |

3.2. Analysis of Water Yield Change in the Ebinur Lake Basin and the Impact of Land-Use Change on Water Yield

From the spatial distribution (Figure 5), water yield in the Ebinur Lake basin from 1995 to 2020 shows a clear high in the northwest and some parts of the southeast. The central and eastern areas are low. Low-grade areas are distributed in clusters, while other graded areas are distributed in bands. The high-gradewater yield areas are mainly concentrated in the upper reaches of the Ulaqsaray, Bortala, and Jinghe rivers, while the low-gradewater yield areas are mainly concentrated in the Kuitun and Gurtu rivers. The highest value in terms of time change occurred in 2010, and the lowest value was in 1995. The total water yield in the Ebinur Lake Basin are ranked as follows: 2010 ($831.12 \times 10^6\text{m}^3$) > 2015 ($706.78 \times 10^6\text{m}^3$) > 2000 ($657.2 \times 10^6\text{m}^3$) > 2005 ($629.4 \times 10^6\text{m}^3$) > 2020 ($567.26 \times 10^6\text{m}^3$) > 1995 ($467.08 \times 10^6\text{m}^3$). Where from 1995 to 2010, water yield increased by $364.04 \times 10^6\text{m}^3$, but from 2010 to 2020, water yield decreased by $263.86 \times 10^6\text{m}^3$, at an annual variation rate of 3.17%. From 1995 to 2020, water yield showed a trend of increase followed by a decrease.

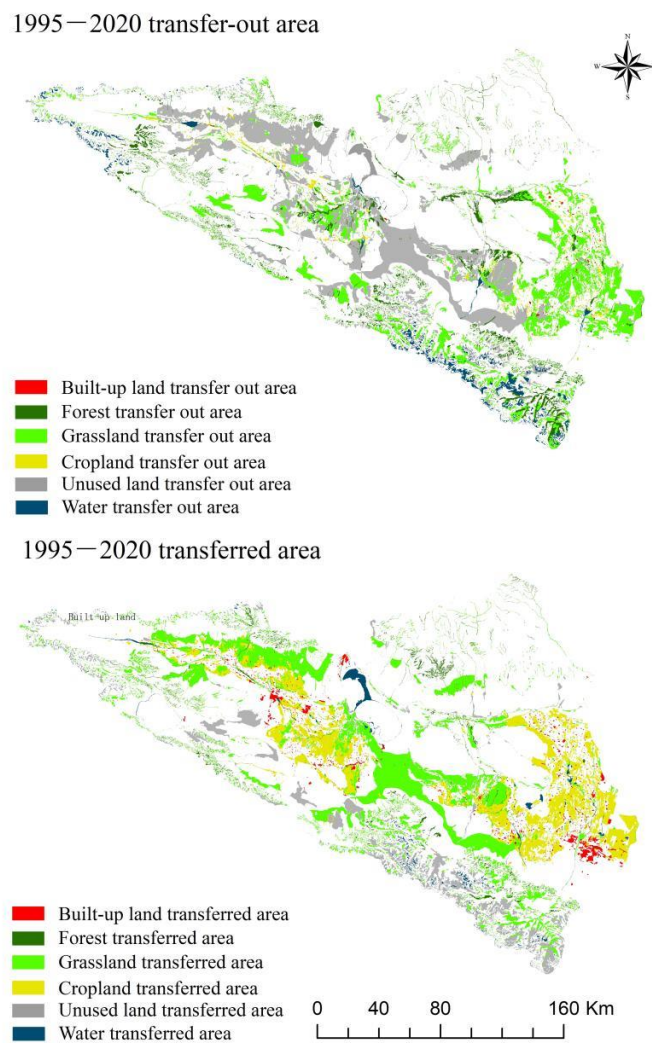


Figure 5. Spatial distribution of land-use transfer-out and transfer-in area of the Ebinur Lake Basin from 1995–2020.

The average water yield of the administrative regions, in descending order, is as follows: Wenquan County > Bole City > Wusu City > Tori County > Jinghe County > Shawan County > Dushanzi District > Karamay District > Kuitun City > Alashankou City. Water yield service function is higher in the northwest and southeast parts of the Ebinur Lake Basin. The central part of the watershed has a lower water yield service capacity, including Alashankou City, Kuitun City, and Karamay District. The total water yield in the Lake Ebinur Basin and water yield service in each region show some consistency in space between different years (Figure 6). In terms of the changes in average water yield of each sub-basin, the average water yield of the Ultaxare River, Boltara River, Jinghe River, and Dahe River along the river system is higher. The highest water yield value is $288.3 \times 10^6 \text{m}^3$. Water yield value is lower in the West Bank Canal, Kuitun River and Gurtu River, and the lowest water yield is up to $1.8 \times 10^6 \text{m}^3$. The average water yield of the remaining sub-basins is $27.2 \times 10^6 \text{m}^3$. The spatial variability between different sub-basins is more obvious. Additionally, the Ultaxare, Bortala, and Jinghe rivers are the main contributing rivers to the average water yield.

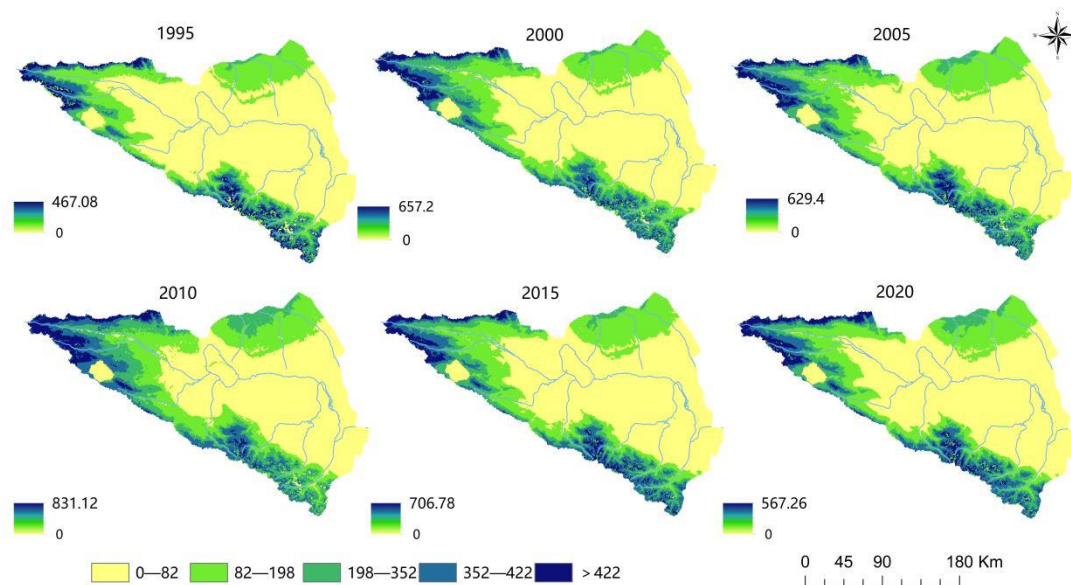


Figure 6. Spatial distribution characteristics of water yield grade in the Ebinur lake Basin.

The area of land-use types and the relationship between the change in water yield and the average depth of water yield in the basin are shown in Figure 7. The values of different land-use types contributing to water yield in the basin, in descending order, are as follows: forest land > grassland > water area > unused land > cropland > built-up land. The area of built-up land and cropland in the Ebinur Lake Basin increases year by year. The area of unused land decreases yearly. The forest land, grassland, and water area have more fluctuations. Additionally, forest land and grassland contribute more to the average water yield and are the main contributing land types. From 1995 to 2010, the major trend in the water yield of cropland, built-up land, and average water yield depth were all increasing and positively correlated. 2010–2020 is a negative correlation. The area of grassland and forest land accounts for 50.23% of the total area of the region, which makes the average multi-year water yield of forest land and grassland higher. The average annual water yield of forest land and grassland is $135.39 \times 10^6 \text{ m}^3$ and $119.31 \times 10^6 \text{ m}^3$, respectively. This finding is followed by cropland and unused land, $96.37 \times 10^6 \text{ m}^3$ and $88.22 \times 10^6 \text{ m}^3$, respectively. Forest land, grassland, and unused land types were negatively correlated with water yield from 1995 to 2010, and the trend was consistent and positive from 2010 to 2020. The trends in water types were consistent and positively correlated only in 1995–2005. The other periods showed the opposite variation. There is a large difference in the relationship between average water yield and type-area change on each land-use type. On the one hand, this difference in the relationship between average water yield and type-area change is due to land-use cover and land-use change. On the other hand, it is closely related to the influence of climate change and human activities on water yield.

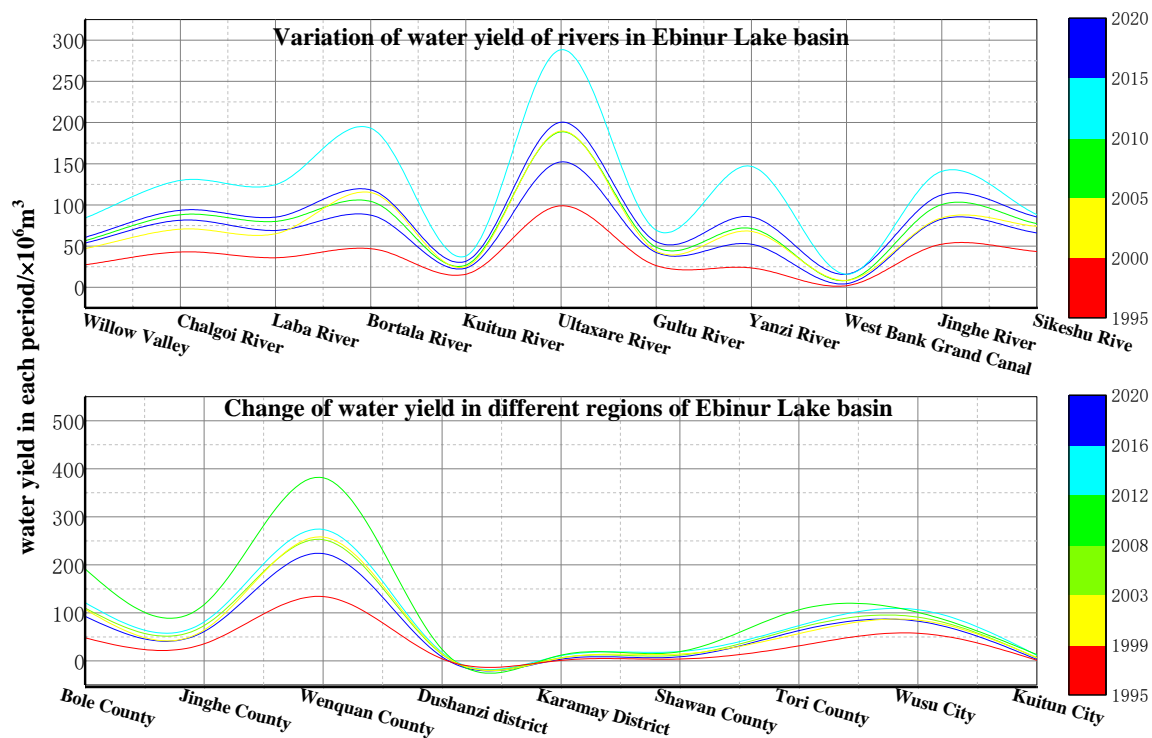


Figure 7. Characteristics of average water yield of each sub-basin and administrative region in the Ebinur Lake Basin.

3.3. Evaluation of Water Purification Service Function and Distribution of Nitrogen and Phosphorus in Different Land-Use Types in the Ebinur Lake Basin

Using the InVEST model water purification module, the water purification service function of the Ebinur Lake Basin from 1995 to 2020 was evaluated (Figure 8). The nitrogen output load of the Ebinur Lake Basin was ranked as follows: 1995 (58.754 kg/ha) > 2000 (57.859 kg/ha) > 2005 (56.749 kg/ha) > 2020 (55.297 kg/ha) > 2015 (54.679 kg/ha) > 2010 (53.206 kg/ha). The average nitrogen export load of the basin decreases significantly from 4.519 kg/ha in 1995 to 4.092 kg/ha in 2010, and then increases slightly to 4.253 kg/ha in 2020. The phosphorus export load of the Lake Ebinur basin is ranked as follows: 1995 (2.176 kg/ha) > 2000 (2.148 kg/ha) > 2005 (2.013 kg/ha) > 2020 (1.679 kg/ha) > 2015 (1.645 kg/ha) > 2010 (1.575 kg/ha). The average phosphorus export load in the basin decreased significantly from 0.167 kg/ha in 1995 to 0.121 kg/ha in 2010, and then increased slightly to 0.129 kg/ha in 2020. The results of the study show that the water quality purification in the Ebinur Lake Basin has a certain consistency between different years. The areas with higher nitrogen and phosphorus output loads and lower water quality purification capacities are concentrated in the northwest and northeast of the basin, including Wenquan County; Bole City; Tori County; and Wusu City. Meanwhile, the areas with lower nitrogen and phosphorus output loads and higher water quality purification capacities are concentrated in the central and eastern parts of the basin, including Jinghe, Kuitun, and Karamay districts. From 1995 to 2010, the output load of nitrogen and phosphorus in the basin of Lake Ebinur decreased and the water quality purification capacity increased. From 2010 to 2020, the output load of nitrogen and phosphorus in the basin of Lake Ebinur increased, while the water quality purification capacity decreased.

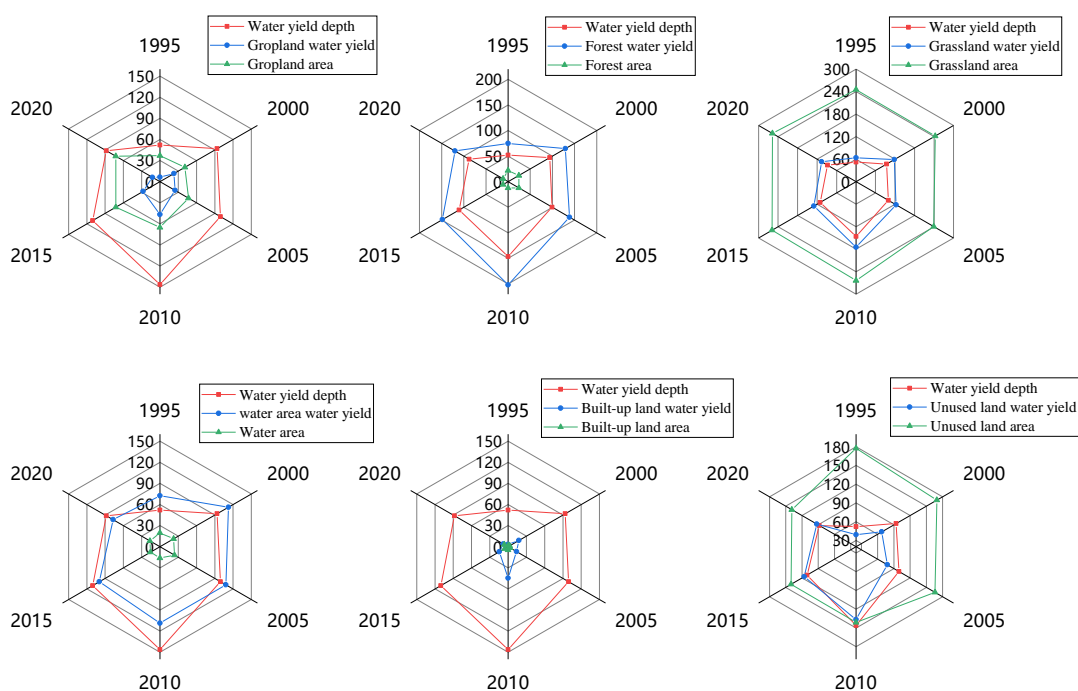


Figure 8. Linkage characteristics of land-use type water yield, type-area change, and average water yield depth.

Cropland contributed the most to nitrogen and phosphorus output, while forest land and basin contributed the least. The main land-use types in the areas with low water purification capacity are cropland and built-up land. This finding indicates that human activities, especially agricultural activities, are the main cause of water environment pollution, perhaps due to the use of large amounts of chemical fertilizers and pesticides in agricultural activities. Therefore, the nitrogen and phosphorus elements that are not absorbed by crops flow directly into the water bodies, which leads to an increase in the output load of nitrogen and phosphorus elements, thus weakening the water purification capacity of the basin. Nitrogen and phosphorus retention on each land-use type in the Ebinur Lake Basin from 1995 to 2020, in descending order, are as follows: cropland > grassland > unused land > built-up land > forest land > water area. The overall amount of nitrogen and phosphorus retention on each land-use type in the basin is increasing, and the overall amount of nitrogen and phosphorus retention on forest land is decreasing. This finding is not consistent with the area change of each land-use type. Land-use change affects the storage and removal efficiency of nutrients such as N and P via vegetation by changing the land-use structure and spatial pattern, affecting basin water quality. The increase in cultivated land and the decrease in forest land degraded the water quality purification function in the study area. In addition, the built-up land and basin area are small, so they have a smaller impact on the water quality purification function in the study area.

3.4. Analysis of Driving Factors of Water Yield and Water Purification Change in the Ebinur Lake Basin

This study was based on the spatial and temporal distributions of water production and water quality services in the Ebinur Lake Basin, combining natural and anthropogenic factors for quantitative research. Using the data for 2020 as an example, the natural and anthropogenic data were gridded using the grid method to create 2098 grid points at a size of 10 km × 10 km within the study area and were used to match water yield and water quality services (detection factor) with influencing factors (explanation factor). The interaction between the various factors and water production and water quality services in the Ebinur Lake Basin, and whether there were significant differences between them, thus revealed the main driving forces influencing the spatial distribution.

From Figure 9a, it can be seen that the different factors, in descending order of q-values of their power to determine water yield, are as follows: PRE (0.91) > TEMP (0.90) > PET (0.83) > Soil (0.68) > LUCC (0.59) > Slope (0.55) > POP (0.27) > NDVI (0.25) > TN (0.18) > GDP (0.08) > TP (0.06) > NTL (0.02). Using the results of factor detection, we can see that the first dominant factor affecting the distribution of spatial variation in water yield is PRE, with a contribution of 0.91. The next factors are TEMP, PET, Soil, and LUCC with equal influence. The rest have relatively small contributions to the spatial variation in water yield. In terms of the magnitude of the interaction produced, TEMP ∩ Slope (0.95), PRE ∩ Slope (0.95), LUCC ∩ PRE (0.95), and LUCC ∩ TEMP (0.94). The interaction between LUCC and TEMP, PET, and PRE types in the study area is evident. The Soil and Slope interaction is more significant compared to the interaction between other factors.

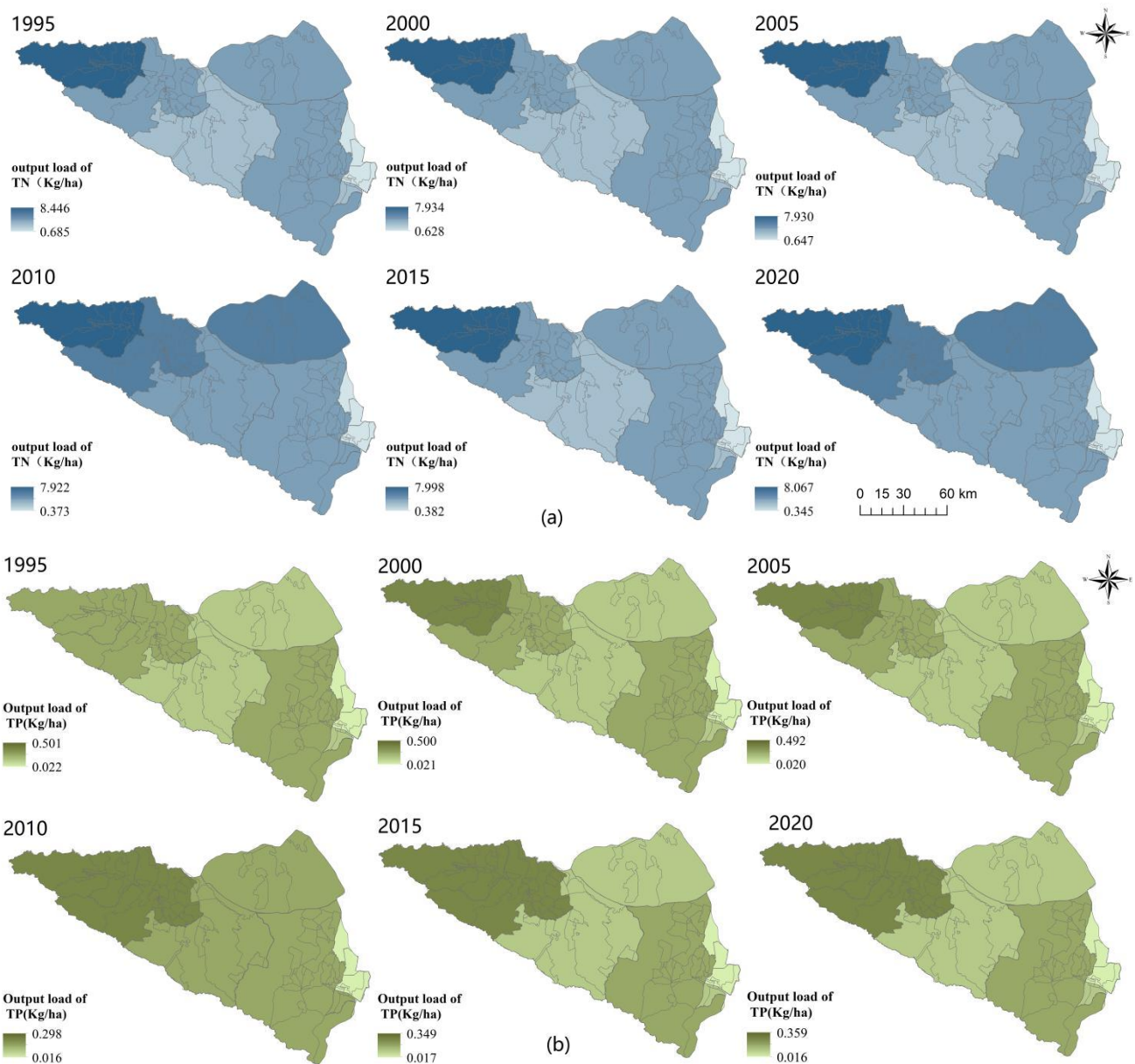


Figure 9. Nitrogen export loads (a) and phosphorus export loads (b) from the Ebinur Lake Basin.

From Figure 9b, the first dominant factor affecting the spatial distribution of water purification is LUCC, with a contribution rate of 0.35, followed by TEMP (0.20). The contribution rate of other factors to the spatial change of water purification is relatively

small. From the perspective of the maximum interaction, the interaction between LUCC and other factors is significant in the study area, including LUCC and WY (0.58), LUCC and POP (0.58), LUCC and PRE (0.57), LUCC and TEMP (0.52), LUCC and PET (0.49), LUCC and Soil (0.46), and LUCC and NDVI (0.44). The interaction between WY and Slope is more significant than that between other factors. The distribution pattern of different ecosystem types is determined by different land-use type structures. The interaction between LUCC factors and other factors is more prominent than that between other factors. This finding fully shows that changes in climate conditions and land-use patterns in the Ebinur Lake Basin have a certain impact on the distribution trend of water yield and water purification (Figure 10). Therefore, it is necessary to strengthen the restoration of ecological projects in the study area, thereby enhancing the ecological service function of the water ecosystem, so as to improve the purification function of water production and water quality in the study area.

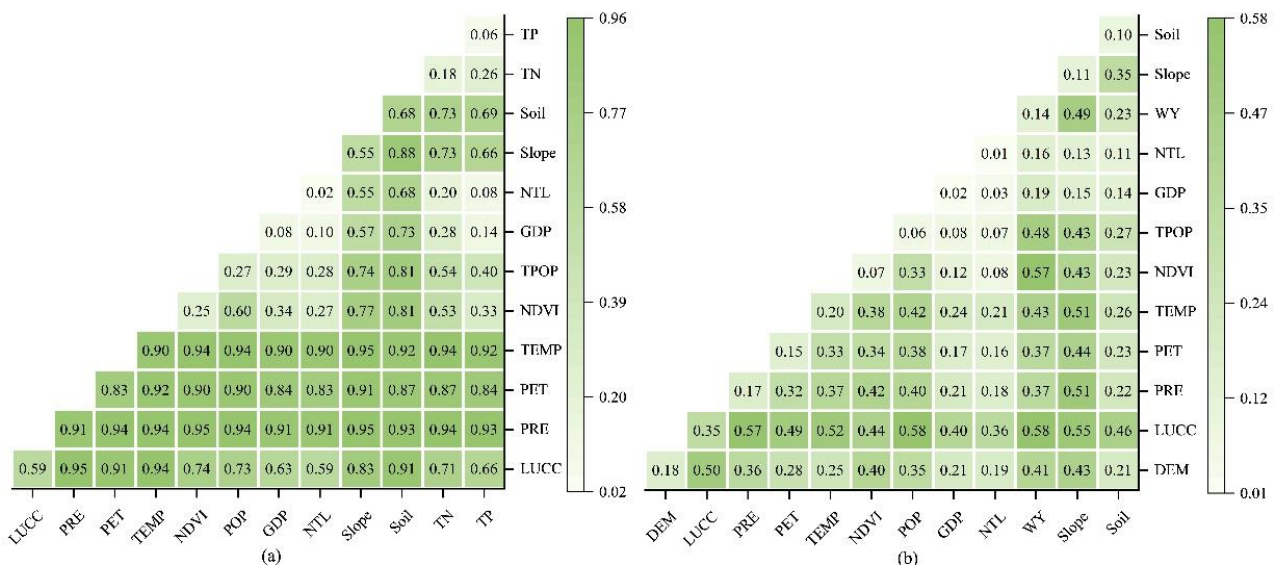


Figure 10. Analysis of the drivers of water yield (a) and water purification (b).

4. Discussion

4.1. Changes in Land Use and Ecosystem Water-Related Functions

Against the background of land-use change, the balance between the water ecological environment and social development in the northwest arid region of China is becoming increasingly unstable, and the water ecological environment will be more likely to be damaged. Appropriate measures should be taken to curb the deterioration of the water’s ecological environment in the northwest arid region. We assessed the impact of land-use change on the provision of two water-related services in the ecosystem of the Ebinur Lake Basin, which is rarely discussed. The results show that land-use change has exerted great pressure on the ability of ecosystems to provide ecosystem services. According to existing research, the impact of climate change on water conservation is greater than that of land-use change on a large scale. For soil output and nutrient output, the impact of land use is greater than that of climate change [38]. On a smaller spatial scale, such as the ecological area investigated in this study, the forest area is decreasing, and land-use change has a greater impact on all water-related ecosystem services.

The results show that the land use in the Ebinur Lake Basin covers a large area of grassland, cultivated land, and unused land, while the area of other land types is relatively small. The construction land and cultivated land are mainly distributed in the west and southeast of the basin, while the forest land and water area are scattered in the basin. The area of construction land and cultivated land in the basin is increasing annually, while the unused land area decreases year by year. The area of forest land, grassland, and water area

fluctuates greatly. From 1995 to 2020, the water yield of the Ebinur Lake Basin increased first and then decreased, and the water production service function was enhanced first and then weakened. The northwest and southeast parts of the basin had high water yield service functions. The change in average water yield in the basin is consistent with that of cultivated land and construction land but inconsistent with that of grassland, forest land, water area, and unused land. Among them, forest land and grassland contribute the most to the water yield. Although the construction land increases year by year, due to the small proportion of the area, the impact on the total water yield is weak, and the contribution to water yield is the lowest. The relationship between the average water yield and the area change of each land-use type is quite different. The output of nitrogen and phosphorus in the Ebinur Lake Basin decreased first and then increased from 1995 to 2020, and the water purification service function of the basin weakened. Areas with high water purification capacity are concentrated in the middle and northeast of the basin, including Jinghe County, Toli County, and Kuitun City. The land-use changes with different nitrogen and phosphorus outputs are consistent with the changes in cultivated land, grassland, water area, construction land, and unused land, but not with the change in forest land. Cultivated land contributed the most to nitrogen and phosphorus output, while forest land and water area contributed the least to nitrogen and phosphorus output. The main types of land use in areas with low water purification capacity are cultivated land and construction land.

4.2. Countermeasures and Impacts

Our method can help identify popular spots of ecosystem service gains and losses and can be used for more intelligent environmental investment decisions. Our maps and comparisons provide a potential tool for determining which regions are most sensitive to land-use change and climate change, enabling us to determine the spatial objectives of investment needs cost-effectively to enhance or restore ecosystem services [39]. Our results show that forest land and grassland, as typical vegetation types, play an important role in implementing major ecological restoration in the Ebinur Lake Basin. Afforestation, conversion of farmland to forest, ecological forest protection, and restoration of degraded grassland have an important impact on the transfer of forest land and grassland. From the perspective of land-use mode, the Ebinur Lake Basin still faces uneven spatial distribution of water production functions due to the difference in land-use allocation, which requires more scientific and reasonable water resource regulation and land-use allocation in the future. At the same time, it is of great significance to pay attention to the role of different sub-basins and reasonably plan and balance the functional positioning of sub-basins for regulating the water production function of the Ebinur Lake Basin. For example, the Ultaxare River, Bortala River, and Jinghe River are basins with the largest contribution to water production, and by balancing reasonable water resource functional zoning based on the different characteristics of water production in different sub-basins, we can further improve the implementation efficiency of regional and macro policies in the future. Agriculture is the main economic development mode in arid areas, and pesticides and fertilizers have become the largest pollution sources. The use of pesticides and fertilizers should be controlled to improve the utilization rate. Protect the quality of water resources, and strengthen the control of pollutants and sewage treatment.

In addition, from science to policy, a clear spatial map of water-related ecosystem services can provide an important basis for landscape policy and management decisions. These maps provide a means to quantify changes in ecosystem services driven by land use and climate factors. In the analysis of our geographical detectors, we showed that the impact of land-use change on soil conservation and nitrogen and phosphorus output is significantly higher than climate change. Our findings show that smart land-use management can improve the ability of ecosystems to provide water-related ecosystem services. To sum up, the analysis framework proposed in this study not only provides an effective tool for identifying popular spots of ecosystem service gains and losses using visual-spatial

maps, but also provides policymakers with a better understanding of how to determine the spatial objectives of investment in a cost-effective manner to strengthen or restore ecosystem services. Our analytical framework also applies to other regions. However, special attention should be paid to the local planning scale, and effective measures should be formulated according to local conditions.

4.3. Research Limitations and Future Studies

The main elements of our method are factor selection, ecosystem service assessment, and factor analysis. Our approach explores the possible impacts of land-use change on two water-related ecosystem services. This method is simple and can be popularized in other regions. The analysis of the main driving factors of water yield and water quality purification by geographical detectors provides a reference for further revealing the driving forces affecting the watershed. Rainfall, potential evapotranspiration, and land-use data have a significant impact on water yield and water quality purification, which can be regarded as direct driving factors affecting water yield and water quality purification services. In addition, soil type, slope, and terrain data, as the main components, also play a significant role. Although this factor is not a direct driving factor, its impact on water production and water purification presents an indirect role, especially since the interaction between other factors is more significant. This factor shows that climate conditions and land use are also the main driving factors. In summary, in the analysis of the leading driving factors of water production and water quality purification, rainfall, potential evapotranspiration, land use, and temperature in the Ebinur Lake Basin were determined to be the main driving forces, while soil type, terrain, and slope were the indirect driving forces. The distinction between the main driving forces and the indirect driving forces has guiding significance for the macro and micro policy guidance of the whole Ebinur Lake Basin and its sub-basins. Despite these advantages, this study also has some limitations. For example, the InVEST cannot include seasonal or monthly fluctuations in nutrient load, which may lead to a potential time-scale mismatch between the InVEST output and management. Another method, time decomposition modeling is needed to solve the impact of time fluctuation runoff on water quality.

5. Conclusions

In order to explore the impact mechanism of human activities on the water ecosystem service functions in the watershed and provide suggestions for land-use decision-makers, this study evaluated the water ecosystem service functions of the Ebinur Lake Basin watershed using the InVEST model and a geographical detector to analyze the relationship with land-use changes. Due to the large proportion of grassland area, the overall change in water yield is more evident than on other lands. Grassland changes play an important role in the water production function of watersheds. The main land-use types in areas with a large change rate of water purification function in the basin are cultivated land and construction land, which shows that human activities, especially agricultural activities, are the main cause of water environment pollution. Therefore, in agricultural production, it is necessary to fertilize rationally and reduce the use of chemical fertilizers. While ensuring the stability of cultivated land, forest land, and grassland should be scientifically and rationally matched to ensure the ecological security of the watershed. The main drivers of changes in water ecosystem services include rainfall, potential evaporation, temperature, and land use. In most of the regions we studied, land-use change had an inhibitory effect on water ecosystem services at the watershed scale. Our study also supports the hypothesis that reasonable land use will have a positive impact on the water production function of the ecosystem to a certain extent, and effective management can help managers formulate more comprehensive spatial planning.

The results of this study reflect the macro evolution trend based on the assessment of water ecosystem services and propose a feasible and replicable framework for land-use decision-making in ecologically fragile areas. The combination of spatiotemporal changes

in land use and geographical detector analysis allows for a more comprehensive assessment of the impact of drivers on ecosystem services. This study not only helps to gain insight into urban growth patterns in the study area but also helps to inform different land-use stakeholders. However, based on the availability of data, this paper does not fully consider the influencing factors and indicators of water quality and only shows limited results, but the research findings are practical, methodological, and policy-relevant. These findings can support the use of ecosystem service information in land planning and the development of more effective ecosystem conservation strategies.

Author Contributions: Conceptualization, Methodology, Formal analysis, Visualization, Writing—original draft, X.D.; Conceptualization, Investigation, Methodology, R.R. and Y.A.; Software, B.W.; Resources, Funding acquisition, Conceptualization, A.K. All authors have read and agreed to the published version of the manuscript.

Funding: This research was funded by the Special Project for Construction of Innovation Environment in Autonomous Region—Construction of Science and Technology Innovation Base (Open Subject of Key Laboratory). Project: Two-way Coupling Process and Mechanism of Urbanization and Water Resources in Bosten Lake Basin (No.2022D04007).

Informed Consent Statement: Informed consent was obtained from all subjects involved in the study.

Data Availability Statement: Data are contained within the article.

Acknowledgments: We thank the two anonymous reviewers for their very constructive comments and suggestions, which have contributed to the improvement of the original manuscript.

Conflicts of Interest: The authors declare no conflict of interest.

References

1. Wu, J.; Li, Y.H.; Huang, L.Y.; Lu, Z.M.; Yu, D.P.; Zhou, L. Spatiotemporal variation of water yield and its driving factors in Northeast China. *Chin. J. Ecol.* **2017**, *36*, 3216–3223.
2. Deng, X.Z.; Zhao, C.H. Identification of water scarcity and providing solutions for adapting to climate changes in the Heihe River Basin of China. *Adv. Meteorol.* **2015**, *2015*, 1–13. [[CrossRef](#)]
3. Xiang, Z.; Junying, W.; Lei, S.; Rong, C.; Zhenxing, Z. A top-down approach to estimate global RO de salination water production considering uncertainty. *Desalination* **2020**, *488*, 114523. [[CrossRef](#)]
4. Leal Filho, W.; Totin, E.; Franke, J.A.; Andrew, S.M.; Abubakar, I.R.; Azadi, H.; Nunn, P.D.; Ouweneel, B.; Williams, P.A.; Simpson, N.P. Understanding responses to climate-related water scarcity in Africa. *Sci. Total Environ.* **2022**, *806*, 150420. [[CrossRef](#)]
5. Návar, J. Fitting rainfall interception models to forest ecosystems of Mexico. *J. Hydrol.* **2017**, *548*, 458–470. [[CrossRef](#)]
6. Mordkovich, V.Z.; Khaskov, M.A.; Naumova, V.A.; De, V.V.; Kulnitskiy, B.A.; Karaeva, A.R. The Importance of Water for Purification of Longer Carbon Nanotubes for Nanocomposite Applications. *J. Compos. Sci.* **2023**, *7*, 79. [[CrossRef](#)]
7. Zhou, G.Y.; Wei, X.H.; Luo, Y.; Zhang, M.F.; Li, Y.L.; Qiao, Y.N.; Liu, H.G.; Wang, C.L. Forest recovery and river discharge at the regional scale of Guangdong Province, China. *Water Resour. Res.* **2010**, *46*, 1–10. [[CrossRef](#)]
8. Ostroumov, S.A. On the biotic self-purification of aquatic ecosystems: Elements of the theory. *Dokl. Biol. Sci.* **2004**, *396*, 206–211. [[CrossRef](#)] [[PubMed](#)]
9. Balda, M.; Mackenzie, K.; Wozidlo, S.; Uhlig, H.; Möllmer, J.; Kopinke, F.-D.; Schüürmann, G.; Georgi, A. Bottom-Up Synthesis of De-Functionalized and Dispersible Carbon Spheres as Colloidal Adsorbent. *Int. J. Mol. Sci.* **2023**, *24*, 3831. [[CrossRef](#)] [[PubMed](#)]
10. Wunder, S.; Engel, S.; Pagiola, S. Taking stock: A comparative analysis of payments for environmental services programs in developed and developing countries. *Ecol. Econ.* **2008**, *65*, 834–852. [[CrossRef](#)]
11. Bastiaanssen, W.G.M.; Karimi, P.; Rebelo, L.M.; Duan, Z.; Senay, G.; Muthuwatte, L.; Smakhtin, V. Earth observation based assessment of the water production and water consumption of Nile Basin agro-ecosystems. *Remote Sens.* **2014**, *6*, 10306–10334. [[CrossRef](#)]
12. An, L.S.; Zhao, Q.S.; Liu, G.Q. Comparative study on representative water quality assessment methods. *Environ. Monit. China* **2010**, *26*, 47–51. [[CrossRef](#)]
13. Beven, K. TOPMODEL: A critique. *Hydrol. Process.* **1997**, *11*, 1069–1085. [[CrossRef](#)]
14. Jayakrishnan, R.; Srinivasan, R.; Santhi, C.; Arnold, J.G. Advances in the application of the SWAT model for water resources management. *Hydrol. Process.* **2005**, *19*, 749–762. [[CrossRef](#)]
15. Boumans, R.; Costanza, R.; Farley, J.; Wilson, M.A.; Portela, R.; Rotmans, J.; Villa, F.; Grasso, M. Modeling the dynamics of the integrated earth system and the value of global ecosystem services using the GUMBO model. *Ecol. Econ.* **2002**, *41*, 529–560. [[CrossRef](#)]
16. Boumans, R.; Roman, J.; Altman, I.; Kaufman, L. The Multiscale Integrated Model of Ecosystem Services (MIMES): Simulating the interactions of coupled human and natural systems. *Ecosyst. Serv.* **2015**, *12*, 30–41. [[CrossRef](#)]

17. Sherrouse, B.C.; Clement, J.M.; Semmens, D.J. A GIS application for assessing, mapping, and quantifying the social values of ecosystem services. *App. Geogr.* **2011**, *31*, 748–760. [[CrossRef](#)]
18. Villa, F.; Ceroni, M.; Bagstad, K.; Johnson, G.; Krivov, S. ARIES (Artificial Intelligence for Ecosystem Services): A new tool for ecosystem services assessment, planning, and valuation. In Proceedings of the 11th Annual BIOECON Conference on Economic Instruments to Enhance the Conservation and Sustainable Use of Biodiversity, Venice, Italy, 21–22 September 2009; pp. 21–22.
19. Ehrlich, P.R.; Kareiva, P.M.; Daily, G.C. Securing natural capital and expanding equity to rescale civilization. *Nature* **2012**, *486*, 68–73. [[CrossRef](#)] [[PubMed](#)]
20. Redhead, J.W.; Stratford, C.; Sharps, K.; Jones, L.; Ziv, G.; Clarke, D.; Oliver, T.H.; Bullock, J.M. Empirical validation of the InVEST water yield ecosystem service model at a national scale. *Sci. Total Environ.* **2016**, *569*, 1418–1426. [[CrossRef](#)] [[PubMed](#)]
21. Keeler, B.L.; Polasky, S.; Brauman, K.A.; Johnson, K.A.; Finlay, J.C.; O’Neill, A.; Kovacs, K.; Dalzell, B. Linking water quality and well-being for improved assessment and valuation of ecosystem services. *Proc. Natl. Acad. Sci. USA* **2012**, *109*, 18619–18624. [[CrossRef](#)]
22. Mulatu, D.W.; van der Veen, A.; van Oel, P.R. Farm households’ preferences for collective and individual actions to improve water-related ecosystem services: The Lake Naivasha basin, Kenya. *Ecosyst. Serv.* **2014**, *7*, 22–33. [[CrossRef](#)]
23. Schmalz, B.; Kruse, M.; Kiesel, J.; Müller, F.; Fohrer, N. Water-related ecosystem services in Western Siberian lowland basins—Analysing and mapping spatial and seasonal effects on regulating services based on ecohydrological modelling results. *Ecol. Indic.* **2016**, *71*, 55–65. [[CrossRef](#)]
24. Lim, C.H.; Song, C.; Choi, Y.; Jeon, S.W.; Lee, W.K. Decoupling of forest water supply and agricultural water demand attributable to deforestation in North Korea. *J. Environ. Manag.* **2019**, *248*, 109256. [[CrossRef](#)]
25. Mei, Y.; Kong, X.H.; Ke, X.L.; Yang, B.H. The impact of cropland balance policy on ecosystem service of water purification—A case study of Wuhan, China. *Water* **2017**, *9*, 620. [[CrossRef](#)]
26. Huang, B.B.; Li, R.N.; Li, R.D.; Zheng, H.; Wang, X.K. Optimization of ecological restoration pattern targeted for water purification improvement in the Baiyangdian watershed, Xiong’an New Area. *Acta Ecol. Sin.* **2020**, *40*, 45–54. [[CrossRef](#)]
27. Liu, J.; Lang, X.D.; Su, J.R.; Liu, W.D.; Liu, H.Y.; Tian, Y. Evaluation of water conservation function in the dry-hot valley area of Jinsha River Basin based on INVEST model. *Acta Ecol. Sin.* **2021**, *41*, 8099–8111. [[CrossRef](#)]
28. Yushanjiang, A.; Zhang, F.; Yu, H.Y. Quantifying the spatial correlations between landscape pattern and ecosystem service value: A case study in Ebinur Lake Basin, Xinjiang, China. *Ecol. Eng.* **2018**, *113*, 94–104. [[CrossRef](#)]
29. Yang, D.; Liu, W.; Tang, L.Y.; Chen, L.; Li, X.Z.; Xu, X.L. Estimation of water provision service for monsoon catchments of South China: Applicability of the InVEST model. *Landsc. Urb. Plann.* **2019**, *182*, 133–143. [[CrossRef](#)]
30. Liang, X.; Guan, Q.F.; Clarke, K.C.; Liu, S.S.; Wang, B.Y.; Yao, Y. Understanding the drivers of sustainable land expansion using a patch-generating land use simulation (PLUS) model: A case study in Wuhan, China. *Comput. Environ. Urb. Syst.* **2021**, *85*, 101569. [[CrossRef](#)]
31. Zhang, X.Y.; Zhang, X.; Li, D.H.; Lu, L.; Yu, H. Multi-scenario simulation of the impact of urban land use change on ecosystem service value in Shenzhen. *Acta Ecol. Sin.* **2022**, *42*, 2086–2097. [[CrossRef](#)]
32. Zhang, L.; Hickel, K.; Dawes, W.R.; Chiew, F.H.S.; Western, A.W.; Briggs, P.R. A rational function approach for estimating mean annual evapotranspiration. *Water Resour. Res.* **2004**, *40*, 1–14. [[CrossRef](#)]
33. Zhou, W.; Liu, G.; Pan, J.; Feng, X. Distribution of available soil water capacity in China. *J. Geogr. Sci.* **2005**, *15*, 3–12. [[CrossRef](#)]
34. Yang, Z.W.; Chen, Y.B.; Qian, Q.L.; Wu, Z.F.; Zheng, Z.H.; Huang, Q.Y. The coupling relationship between construction land expansion and high-temperature area expansion in China’s three major urban agglomerations. *Int. J. Remote Sens.* **2019**, *40*, 6680–6699. [[CrossRef](#)]
35. Liu, J.; Xu, Q.L.; Yi, J.H.; Huang, X. Analysis of the heterogeneity of urban expansion landscape patterns and driving factors based on a combined Multi-Order Adjacency Index and Geodetector model. *Ecol. Indic.* **2022**, *136*, 108655. [[CrossRef](#)]
36. Han, Y.; Zhang, Y. Spatiotemporal variations of county economies and influencing factors: A case study of Gansu Province. *J. Geo Inform. Sci.* **2019**, *21*, 1735–1744. [[CrossRef](#)]
37. Yin, S.G.; Li, Z.J.; Song, W.X.; Ma, Z. Spatial differentiation and influence factors of residential rent in Nanjing based on geographical detector. *J. Geo. Inf. Sci.* **2018**, *20*, 1139–1149. [[CrossRef](#)]
38. Yang, F.S.; Yang, X.M.; Wang, Z.H.; Qi, W.J.; Li, Z.; Meng, F. Geographic detection of impact factors of economic differences among typical counties in Jiangxi Province. *J. Geo. Inform. Sci.* **2018**, *20*, 79–88. [[CrossRef](#)]
39. Wang, D.Q.; Pang, X.Q. Research on green land-use efficiency of Beijing-Tianjin-Hebei urban agglomeration. *China Popul. Resour. Environ.* **2019**, *29*, 68–76. [[CrossRef](#)]
40. Bai, Y.; Ochuodho, T.O.; Yang, J. Impact of land use and climate change on water-related ecosystem services in Kentucky, USA. *Ecol. Indic.* **2019**, *102*, 51–64. [[CrossRef](#)]
41. Hoyer, R.; Chang, H. Assessment of freshwater ecosystem services in the Tualatin and Yamhill basins under climate change and urbanization. *Appl. Geogr.* **2014**, *53*, 402–416. [[CrossRef](#)]

Disclaimer/Publisher’s Note: The statements, opinions and data contained in all publications are solely those of the individual author(s) and contributor(s) and not of MDPI and/or the editor(s). MDPI and/or the editor(s) disclaim responsibility for any injury to people or property resulting from any ideas, methods, instructions or products referred to in the content.